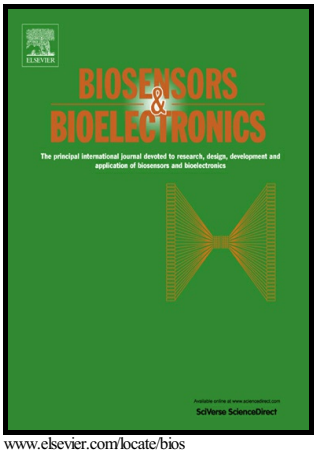

www.elsevier.com/locate/bios

Molybdenum Disulfide Field-Effect Transistor Biosensor for Ultrasensitive Detection of DNA by Employing Morpholino as Probe

Junchi Mei, Yu-Tao Li, Hong Zhang, Meng-Meng Xiao, Yong Ning, Zhi-Yong Zhang, Guo-Jun Zhang

PII: S0956-5663(18)30215-X
DOI: https://doi.org/10.1016/j.bios.2018.03.043
Reference: BIOS10369

To appear in: *Biosensors and Bioelectronic*

Received date: 15 January 2018
Revised date: 14 March 2018
Accepted date: 19 March 2018

Cite this article as: Junchi Mei, Yu-Tao Li, Hong Zhang, Meng-Meng Xiao, Yong Ning, Zhi-Yong Zhang and Guo-Jun Zhang, Molybdenum Disulfide Field-Effect Transistor Biosensor for Ultrasensitive Detection of DNA by Employing Morpholino as Probe, *Biosensors and Bioelectronic,* https://doi.org/10.1016/j.bios.2018.03.043

Molybdenum Disulfide Field-Effect Transistor Biosensor for Ultrasensitive Detection of DNA by Employing Morpholino as Probe

Junchi Mei[1], Yu-Tao Li[1], Hong Zhang[2], Meng-Meng Xiao[3], Yong Ning[1], Zhi-Yong Zhang[3,*], Guo-Jun Zhang[1,*]

[1]School of Laboratory Medicine, Hubei University of Chinese Medicine, 1 Huangjia Lake West Road, Wuhan 430065, P.R. China

[2] Teaching and Research Office of Forensic Medicine, Hubei University of Chinese Medicine, 1 Huangjia Lake West Road, Wuhan 430065, China

[3]Key Laboratory for the Physics and Chemistry of Nanodevices, Department of Electronics, Peking University, No.5 Yiheyuan Road Haidian District, Beijing 100871, P.R. China

[*]Corresponding author: Tel: +86-27-68890259, Fax: +86-27-68890259

E-mail: zhanggj@hbtcm.edu.cn; zyzhang@pku.edu.cn

Abstract

This work reports on a molybdenum disulfide (MoS_2) based field-effect transistor (FET) biosensor for ultrasensitive label-free detection of DNA via phosphorodiamidate morpholino oligos (PMO)-DNA hybridization. After the chip was fabricated and the sensing channel was modified with positive charges, the negatively charged MoS_2 nanosheet was drop-casted onto the channel, enabling MoS_2 to tightly bind to the sensing surface via electrostatic interactions. Meanwhile, DNA analogue, PMO, was immobilized on the MoS_2 surface, and detection of PMO-DNA hybridization was conducted by the fabricated MoS_2 FET biosensor. Due to the neutral character and high affinity of PMO, a limit of detection (LOD) down to 6 fM was obtained, which is lower than that of the previously reported MoS_2 FET DNA biosensor based on DNA-DNA hybridization. In addition, the MoS_2 FET biosensor also showed high sequence specificity capable of distinguishing the complementary DNA from one-base mismatched DNA, three-base mismatched DNA and noncomplementary DNA. Moreover, the unique FET biosensor was able to detect DNA in complex sample like serum, making the method potential in disease diagnostics.

Keywords: Molybdenum disulfide; Phosphorodiamidate morpholino oligos; Field-effect transistor biosensor; DNA; Detection

1. Introduction

DNA, as one of the most important genetic materials, plays a significant role in life science (Watson and Crick 1953). DNA detection is critical in many fields (such as disease diagnosis, forensic investigation, genomics, etc), especially in the field of early diagnosis of cancer and infectious diseases (Bryant et al. 2004; Sozzi et al. 1999; Yager et al. 2008). Hence, it is urgent to develop sensitive, selective and rapid DNA assays due to the ever-increasing clinical expectation (Bryant et al. 2004; Drummond et al. 2003; Du and Dong 2016; Sassolas et al. 2008; Turner 2013).

So far, a series of methods based on nanomaterials (Tan et al. 2017; Wang et al. 2012; Zhang 2015), such as nanoparticles (Cai et al. 2015), carbon nanotubes (CNTs) (Wang 2005), silicon nanowires (SiNWs)(Peng et al. 2014), nanobelts (Pan et al. 2001), graphene oxide (GO) (Cai et al. 2014; Sanchez et al. 2011; Zheng et al. 2015) and molybdenum disulfide (MoS_2)(Ha et al. 2014; Radisavljevic et al. 2011; Sarkar et al. 2014) have been developed for sensitive and selective detection of DNA, including fluorescence assays (Ha et al. 2014), colorimetric assays (Yuan et al. 2014), electrochemical assays (Drummond et al. 2003; Wang 2003; Wu et al. 2012) and electrical assays (Kawde and Wang 2004). Among them, the label-free field-effect transistor (FET) biosensors utilizing nanomaterials have recently attracted much attention because of their high selectivity and sensitivity.

FET biosensors with CNTs have been extensively studied and they have shown effective detection of DNA at the nanomolar (nM) level (Kim et al. 2012). In the past few years, nanoelectronic devices based on SiNWs or reduced graphene oxide (rGO) have been also used for electrical detection of protein and DNA molecules due to many of their interesting and unique properties (Chen et al. 2013; Li et al. 2004). Recently, another promising nanomaterial candidate for FET biosensors as a sensing interface is molybdenum disulfide (MoS_2)(Sarkar et al. 2014). With the unique properties of layered sandwich structures, high on/off current ratio and high flexibility (Gan et al. 2017; Mak et al. 2010; Radisavljevic et al. 2011), MoS_2 nanosheet has been used to establish FET biosensor increasingly. Yang et al. (Yang et al. 2014) reported a label-free sensitive biosensor platform for cancer marker protein detection with high sensitivity by using multi-layer MoS_2 as the sensing interface. Banerjee et al. (Banerjee et al. 2014) fabricated a FET biosensor based on MoS_2 for detecting pH and specific protein. Johnson et al. (Johnson et al. 2016) developed wafer-scale, high-yield fabrication of monolayer MoS_2-based biosensors for protein detection. Lee et al. (Lee et al. 2015) constructed the FET biosensors based on chemically synthesized MoS_2 for label-free electrical detection of DNA-DNA hybridization.

Compared to DNA probe, phosphorodiamidate morpholino oligos (PMO), belonging to the third generation of antisense oligonucleotides (Summerton 1989), enables a low noise and high sensitivity detection of DNA because it holds a neutral backbone of morpholine rings and makes a weak impact on their hybridization

behavior between PMO and DNA (Summerton and WELLER 1997; Summerton 2006). Recently, Zhang et al. (Zhang et al. 2010) demonstrated PMO-functionalized SiNW biosensor for the sequence-specific detection of DNA based on PMO-DNA hybridization. Very recently, Liao et al. (Liao et al. 2017) reported a very simple method to fabricate a novel PMO-modified nanochannel-based biosensor for miRNA detection in serum sample. Nevertheless, such a unique PMO probe has yet been applied to the MoS_2-based FET biosensor for DNA detection.

In this work, we first develop a MoS_2-based FET biosensor for sensitive and specific detection of DNA based on PMO-DNA hybridization. MoS_2 nanosheet is drop-casted onto the fabricated FET device. Prior to the drop-casting, 3-aminopropyltriethoxysilane (APTES) is used to modify the sensing channel with positive charges, enabling an efficient binding between Si surface and MoS_2 via electrostatic interaction (Wu et al. 2012). Such an attempt is to enhance a strong contact on the sensing interface, avoiding a leakage. Specially, the PMO-DNA hybridization is conducted to determine gene sequence by immobilizing PMO on the MoS_2 surface. With unique properties of MoS_2 as the sensing interface and PMO as the probe molecule, ultrasensitive detection of PMO-DNA hybridization based on the MoS_2-based FET biosensor is achieved. Moreover, the MoS_2-based FET biosensor is capable of distinguishing a single base mismatched sequence. As a result, such a novel sensing platform is potentially used as a point-of-care testing tool for disease diagnosis.

2. Experimental Section

2.1 Materials. The length of PMO and DNA sequences is 22 base pairs, respectively. The sequence of the PMO probe is 5′-H_2N-AACCACACAACCTACTACCTCA-3′. The sequences of DNA are 5′-TGAGGTAGTAGGTTGTGTGGTT-3′ (complementary), 5′-CY3-TGAGGTAGTAGGTTGTGTGGTT-3′ (complementary, fluorescence-labeled), 5′-TGAGGTAGTAGGTTGTATGGTT-3′ (one-base mismatched), 5′-TGAGGTTGTTGGT-TGTATGGTT-3′ (three-base mismatched) and 5′-TAGCTTATCAGACTGATGTTGA-3′ (noncomplementary). PMO was purchased from Gene Tools LLC (Philomath, OR, USA). DNAs were purchased from Sangon Biotech Co. Ltd. (Shanghai, China). MoS_2 suspension (1mg/mL) was purchased from XF Nano Co. Ltd. (Nanjing, China). 1-Pyrenebutanoic acid succinimidyl ester (PASE), 3-Aminopropyltriethoxysilane (APTES) and ethanolamine (EA) were ordered from Sigma-Aldrich (St. Louis, MO, USA). Ultrapure water obtained from a Millipore water purification system (18.2 MΩ resistivity, Milli-Q Direct 8) was used throughout the research.

2.2 Fabrication of MoS_2 FET Biosensors. The fabrication of the FET biosensor chip was completed by using the standard semiconductor technology. The gold electrodes were fabricated on SiO_2 (285 nm)/Si substrate to make source and drain electrodes using conventional macro-nano processing technologies including photolithography and electron-beam evaporation. The size of the whole device is 6-4.5 mm. The electrodes (50 nm thick) are 4 μm apart. To enhance the adhesion between Au and Si wafer, a 5 nm thick Ti layer was used. Then, the chip was immersed in the 2% APTES solution for 2 h. After that, the diluted MoS_2 suspension was drop-casted onto the nanochannel and was immersed in the DI water and sonicated for 30 s to obtain few-

layer MoS_2, followed by thoroughly washing with DI water and drying with nitrogen (N_2).

2.3 Immobilization of PMO on the MoS_2 Surface. In order to immobilize PMO on the MoS_2 surface, a cross-linker molecule, PASE was used. The MoS_2 FET was treated with a 5 mM PASE in dimethyl-sulfoxide (DMSO) for 1 h at room temperature and washed with pure DMSO, ethanol, and DI water, respectively. The PASE-modified FET was treated with 10 μM PMO for 2 h at room temperature followed by being rinsed in sequence with 0.5×PBS containing 0.2% SDS, 0.5×PBS, and DI water, respectively, to remove the unreacted probe. The device was then incubated with 100 mM ethanolamine solution (pH 9.0) for 1 h to prevent possible nonspecific binding events and then rinsed by DI water.

2.4 Hybridization. PMO-DNA hybridization was conducted by dropping an appropriate concentration of complementary target DNA solution onto the device and incubated for 1 h. Then the chip was rinsed in sequence with 0.5×PBS containing 0.2% SDS, 0.5×PBS, and DI water, respectively, to remove the unhybridized DNA sequence and dried with N_2. The same procedure was repeated by using the one-base mismatched and noncomplementary DNA sequences instead of the complementary target DNA sequence to perform the hybridization with the PMO probe.

2.5 Denaturation of PMO-DNA duplex. After PMO-DNA hybridization, **t**he denaturation was performed by immersing the FET chip in 8.3 mol/L Urea solution for 5 min at room temperature. After that, the chip was rinsed by DI water and dried with N_2.

2.6 Electrical Measurements. The liquid-gated MoS_2 FET devices were measured in a semiconductor parameter analyzer (Keithley 4200-SCS) coupled with a probe

station (EverBeing BD-6). For I_{ds}-V_g (I_{ds} is the drain-source current, V_g is the gate voltage) curve measurements of the devices, a silver wire was used as a gate electrode and a constant bias V_{ds} = 0.1V (the drain-source voltage) was applied. I_{ds}-V_{ds} curves were measured at an assigned V_g value.

2.7 Characterization. A UltraPlus scanning electron microscopy (SEM) (Carl Zeiss, Japan) was used for SEM characterization of the device at a 5 kV acceleration voltage. Atomic force microscopy (AFM) was conducted with a SPM9700 AFM (Shimadzu, Japan). The fluorescence characterization of PMO-DNA hybridization was obtained by fluorescence microscope Olympus DP72 (Olympus, Japan). Both transmission electron microscopy (TEM) and dynamic light scattering (DLS) measurements were performed on the MoS_2 suspension by JEM-2100 (JEOL, Japan) and Zetasizer Nano ZSP (Malvern Panalytical Ltd., British)

3. Results and Discussion

3.1 Working principle. Figure 1 shows the working principle of the MoS_2 FET sensors for PMO-DNA hybridization. As illustrated, the FET device is fabricated on a SiO_2/Si substrate by the conventional macro-nano processing technologies. The FET channel surface is functionalized with APTES with an attempt to obtain a positively charged surface. Subsequently, MoS_2 suspension is drop-casted onto the channel to contact source and drain electrode. Because MoS_2 is negatively charged, MoS_2 can be anchored onto the channel surface tightly through electrostatic interactions, which is extremely important for effectively contructing MoS_2 layers on the SiO_2 surface. PASE (the linker molecule) is then fixed on the MoS_2 surface though π-π coordination interaction between the MoS_2 surface and the pyrene group (Huang et al. 2016). The

PMO probe is immobilized on the MoS_2 surface through the covalently bond between the amino group on PMO and an amide bond on the other end of PASE, after which ethanolamine is used to prevent possible nonspecific adsorption. It is obvious that some unreacted imide bond is still exposed on the chip surface. By using ethanolamine as the blocking agent, the tail end of ethanolamine, amino groups, can react with excess terminus of PASE. Finally, the target DNAs are applied onto the device for hybridization with probe PMO. The sensing signal was recorded by monitoring the electrical conductivity change of the MoS_2 FET sensor.

3.2 Characterization of MoS_2 nanosheets. To clarify the characterization of MoS_2, both TEM and DLS measurements were performed on the MoS_2 suspension, respectively. Figure S1 shows TEM image of the well-exfoliated few layer MoS_2 nanosheets. It was found that the average lateral sizes of MoS_2 nanosheets were larger than 200 nm. Figure S2 presents DLS image of MoS_2 suspension. It was clearly seen that a strong peak was around 211 nm, meaning that the average diameter of MoS_2 nanosheet is 211 nm. Figure S2b shows Zeta potential distribution of MoS_2 flake. The average Zeta potential of MoS_2 was found to be -40 mV, further demonstrating that the MoS_2 suspension is stable and not aggregated. At the same time, the surface of MoS_2 was proved to be negatively charged. The results are consistent with the reported literature (Song et al. 2014).

To visualize the nanosheet morphology assembled on the sensing channel, both SEM and AFM were employed for characterization. The SEM image in Figure 2a clearly shows that few-layer MoS_2 nanosheet spanned across a pair of Au electrodes and the lateral sizes of the nanosheet were appropriately between 200-1000 nm. The AFM image in Figure 2b further shows the structures of the MoS_2 inside the channel. It was observed that the MoS_2 sheet connected a pair of Au electrodes. And based on

the height profiles, the thickness of the MoS_2 sheet was appropriately between 5-25nm, revealing few-layered structures. To sum up, the MoS_2 nanosheet has been localized between source and drain electrodes, and the MoS_2 FET biosensor has successfully been fabricated as expected.

3.3 Electrical properties of MoS_2 FET device. The electrical properties of the MoS_2-based FET device were characterized by measuring current-voltage (I-V) curves. As shown in Figure 3, the transfer characteristic curves and the output characteristic curves of the device were measured by the MoS_2 FET devices, respectively. The FET transfer characteristics in Figure 3a clearly indicate that the MoS_2 FET device was p-type. Note that the p-type MoS_2 device is different from those n-type MoS_2 devices, in which MoS_2 was grown by CVD or produced by mechanical exfoliation. The reason may be explained by the fact that the device was converted to p-type semiconductor when exposed to an oxygen-containing atmosphere (Zeng et al. 2011; Zhou et al. 2016). In such a case, oxygen molecules were adsorbed onto defects or sulfur sites on the top layer of the MoS_2 film, working as p-type dopants for the MoS_2 surface. Moreover, the output characteristics curves show that the drain current decreased when the gate voltage was increased from 0 to 0.3 V in steps of 0.1 V in Figure 3b, further indicating that the whole device is p-type. The result also indicates an ohmic contact between the MoS_2 film and the Au electrodes.

3.4 Fluorescent confirmation of PMO-DNA hybridization on MoS_2 surface. In order to confirm the successful surface modification of PMO probe on the MoS_2 surface, target DNA labeled with fluorescent dye (Cy3) was applied to the PMO-activated silicon surface. The hybridization between PMO probe and Cy3-labeled target DNA was confirmed by fluorescence microscope. As shown in Figure S3, an

obvious fluorescence was observed when Cy3-labeled target DNA was applied to PMO functionalized MoS_2 surface. As a control, a negligible signal was seen when Cy3-labeled target DNA was applied to the MoS_2 surface, on which PMO probe was not functionalized (Figure S3b). These results exhibit that PMO probe immobilization on the MoS_2 surface is successful.

3.5 Sensitivity. The sensitivity of the MoS_2 FET biosensor was investigated by hybridization of various concentrations of complementary DNAs with the PMO-functionalized MoS_2 FET device. As seen from Figure 4a, the I_{ds} of the device decreased with increased concentration of the complementary DNA from 10 fM to 1 nM. In order to effectively analyze the data, a quantification method reported by Nam et al. (Nam et al. 2015) and Anand et al. (Anand et al.) was chosen. Inset shows the I_{ds} measured under a given V_g(V_g=-0.1~0.1V) in the linear regime with the various concentrations, in which all curves are parallel. So I_{ds} was defined as the current between drain and source in case of V_g=0 V. Through normalization, the $\Delta I_{ds}/I_{ds0}$ (namely, the rate of change of I_{ds} after hybridizing with different concentrations of complementary DNA relative to I_{ds} of PMO) was acquired. Figure 4b shows a linear response between the logarithmic value of DNA concentration defined as lgC and the drain current change. The linear relationship was represented by $\Delta I_{ds}/I_{ds0}(\%) = 3.69\ lgC_{DNA}(fM) + 1.58$ (R^2=0.9966), clearly revealing that the current decreased along with the increasing DNA concentrations. Dashed line in Figure 4b represents the noise level (4.5%) from the blank control test. Then, the limit of detection (LOD) as low as 6 fM was achieved based on the signal that exceeds the background by 3-fold. Lee et al. (Lee et al. 2015) demonstrated specific sequence detection by DNA-modified carbon nanotube FET with detection limit of 1 nM. Chen et al. (Chen et al.

2013) also reported sequence-specific DNA sensors based on SiNWs, in which the single stranded probe DNA molecules was immobilized on the nanowire surfaces and the LOD down to 25 pM was obtained. Zhang et al. (Zhang et al. 2015) also demonstrated a SiNW biosensor for DNA detection, in which PMO was functionalized on the SiNW surface, and DNA concentration as low as 100 fM could be detected. Chen et al. (Chen et al. 2013) explored a liquid-gated, single-layer graphene biosensor for detection of DNA hybridization and achieved a LOD as low as 1 pM. Cai et al. (Cai et al. 2014) reported a graphene FET DNA biosensor by utilizing peptide nucleic acid as probe. In this work, a detection limit of 100 fM was obtained. Recently, Lee et al. (Lee et al. 2015) fabricated a CVD-grown MoS_2 FET device for DNA detection, in which DNA was employed as probe and the low LOD (10 fM) was achieved. The performance comparison among various FET DNA biosensors is shown in Table S1. As observed, the MoS_2 FET biosensor developed in this work exhibits the highest sensitivity (6 fM), which is probably caused by usage of the MoS_2 nanochannel as conducting materials and PMO as probe molecule.

On the other hand, it is tough to precisely control the thickness of MoS_2 layer within the channel because the MoS_2 layer is deposited by drop-casting. However, the average thickness of different batches of devices was observed to be around 5-25 nm when the same concentration of MoS_2 suspension (0.5 mg/mL) was drop-casted on the chip and further treatment like sonication was applied. It is clear that different thickness of MoS_2 can affect the detection sensitivity and reproducibility of sensor fabrication. Thus, we fabricated 5 batches of MoS_2 FET devices and conducted the corresponding AFM images. Meanwhile, detection sensitivities of these 5 MoS_2 FET devices were also performed for comparison. It is seen from Table S2 that the LODs of the 5 devices are in the same order of magnitude although the thickness of the

different MoS_2 FET devices is varying. This means that the fabricated MoS_2 FET devices have satisfactory reproducibility.

3.6 Specificity. To verify the specificity of the MoS_2 FET biosensor, 1 nM non-complementary DNA, 1 nM one-base mismatched DNA, 1 nM three-base mismatched DNA and 1 pM complementary DNA were applied to the PMO-functionalized MoS_2 FET devices, respectively. As shown in Figure 5, the $\Delta I_{ds}/I_{ds0}$ of non-complementary and three-base mismatched DNA was found to be negligible. It is probably that the signal was caused by nonspecific adsorption. Nevertheless, the $\Delta I_{ds}/I_{ds0}$ of complementary DNA was remarkably observed. On the other hand, when one-base mismatched DNA was hybridized to the PMO functionalized MoS_2 FET biosensor, the $\Delta I_{ds}/I_{ds0}$ was observed to be larger than that of non-complementary and three-base mismatched DNA, and smaller than that of complementary DNA. This is probably because the formed duplex between the one-base mismatched DNA and the probe PMO is unstable and it may be melted during the washing steps. The result is in good agreement with the previously reported results. The results confirm that the MoS_2 FET biosensors can distinguish the complementary DNA from one-base mismatched DNA, three-base mismatched DNA and noncomplementary DNA. It is clear that the developed biosensor can be used for SNP detection.

3.7 Repeatability and Stability. The repeatability and stability of the MoS_2 FET biosensor were also investigated. The repeatability was conducted by carrying out hybridization and dehybridization between PMO and target DNA. As clearly seen in Figure S4a, after three cycles of denaturation and rehybridization, the hybridization signal percentages of the second and third hybridizations were found to be 88% and

80% of the first-cycle hybridization signal, respectively, indicating that the MoS_2 FET biosensor have a satisfactory repeatability and the device could be re-used multiple times.

Afterwards, the stability of the MoS_2 biosensor was evaluated by storing the device in a vacuum oven for a period of times and detecting its electrical properties. As shown in Figure S4b, the $\Delta I_{ds}/I_{ds0}$ retained more than 92% of its original value over 7 days. Even after 15 days, it still kept 86% of its original value. This signal decrease is probably because of nonspecific adsorptions caused by air and water in environment.

3.8 Serum sample analysis. Real sample detection is a critical aspect to evaluate a biosensor. To do so, the MoS_2 FET biosensor was used for detecting target complementary DNA in serum samples. The complementary DNA was spiked to 10× diluted healthy human serum and different concentrations of DNA in serum were prepared. In the experiment, two different concentrations of DNA in serum (10 fM and 1 pM) for DNA detection were chosen for positive control, while 10×diluted serum without target DNA was used as blank control. As illustrated in Fig. 6, the $\Delta I_{ds}/I_{ds0}$ of 1 pM DNA in serum was higher than that of 10 fM DNA in serum. Furthermore, it was observed that the $\Delta I_{ds}/I_{ds0}$ of serum with DNA was larger than that of serum without DNA. Thus, it is proven that the MoS_2 FET biosensor shows potential application in detecting DNA in real samples

3.9 Potential application as a POCT device. Recently, increasing researchers turn to develop integrated sensors to make the DNA detection practical (Tang et al. 2017a). Choi et al. (Choi et al. 2016; Choi et al. 2017) showed an integrated paper-based

biosensor for nucleic acid testing for the purpose of constructing a POCT device, which involves three necessary parts including extraction, detection and readout. Next, Tang et al. (Tang et al. 2017b) reported a fully disposable and integrated paper-based device for nucleic acid extraction, amplification and detection. Comparing with other integrated devices, that device decreases the cost, reduces the operation step and realizes the fully portable and disposable feature. In addition, for analysing multiple samples faster, the high-throughput capability, automatic and integrated rotary microdevice is demonstrated by Park et al. (Park et al. 2017). Similar to the above-mentioned great work, a sample-in and answer-out microsystem will potentially be developed by integrating silicon chip-based nucleic acid extraction and PCR for DNA sources, MoS_2 FET device sensor for detection, and electrical circuits for readout together, pointing to a POCT device development.

Cost is another issue for the practical applications. In this work, a 4-inch wafer was used to fabricate the FET devices, on which 110 single FET devices were made. Roughly, one 4-inch silicon wafer costs ~30 USD. Meanwhile, 200 mL of 1 mg/mL MoS_2 only costs 85 USD. If 10 μL of MoS_2 is drop-casted on the chip, the cost can be negligible. The fabrication fee for one chip is approximately 700 USD. This means that one FET device finally costs ~7 USD. As known, the chip cost can deeply go down if the chip is fabricated for potential mass production in silicon foundries.

4. Conclusions

In summary, the PMO-modified MoS_2 FET biosensor for detecting DNA based on PMO-DNA hybridization with high sensitivity and specificity has been developed. Because the neutral PMO was used as probe, the PMO-modified MoS_2 FET biosensor

showed both high sensitivity and specificity. The MoS_2 FET biosensor also exhibited a capability of reusability and stability, which is cost-effective for future real applications. What's more, the developed biosensor was also able to detect target DNA in serum sample. All of these advantages indicate that this work provides a new strategy for DNA analysis, which can find its potential applications in disease diagnostics as a POCT tool. Nevertheless, the limitations of this work lie in the following aspects: 1) the size of the MoS_2 nanosheet is not larger enough (less than 1000 nm), making FET channel contact difficult; 2) due to the drop-casting fabrication, the MoS_2 nanosheet inside the sensing channel is relatively rough, but the thickness can be controlled within a certain range; 3) similar to other DNA biosensors, both orientation of PMO probe and PMO-DNA hybridization efficiency are hard to control. In the future, efforts in our laboratory are made to realize a precisely controllable MoS_2 FET biosensor with high reproducibilty. Based on this, an electrical biosensor detection module consisting of the MoS_2 FET biosensor and a miniaturized readout system is hopefully constructed, offering an integrated and portable platform to enable gene profiling and molecular diagnostics.

Acknowledgements

This work was supported by the National Natural Science Foundation of China (Nos. 21475034, 21675041, and 61390504).

Supporting Information

Supplementary data associated with this article can be found in the online version at …

References:

Anand, A.; Liu, C.; Chou, A.; Hsu, W.; Ulaganathan, R. K.; Lin, Y.; Dai, C.; Tseng, F.; Pan, C.; Chen, Y. , 2017. ACS Sens. 2, 69-79.

Bryant, P.A., Venter, D., Robins-Browne, R., Curtis, N., 2004. Lancet Infect. Dis. 4(2), 100-111.

Cai, B., Huang, L., Zhang, H., Sun, Z., Zhang, Z., Zhang, G., 2015. Biosens. Bioelectron. 74, 329-334.

Cai, B., Wang, S., Huang, L., Ning, Y., Zhang, Z., Zhang, G., 2014. ACS Nano 8(3), 2632-2638.

Chen, T., Loan, P.T.K., Hsu, C., Lee, Y., Tse-Wei Wang, J., Wei, K., Lin, C., Li, L., 2013. Biosens. Bioelectron. 41, 103-109.

Choi, J.R., Hu, J., Tang, R., Gong, Y., Feng, S., Ren, H., Wen, T., Li, X., Abas, W.A.B.W., Pingguan-Murphy, B., 2016. Lab Chip. 16(3), 611-621.

Choi, J.R., Yong, K.W., Tang, R., Gong, Y., Wen, T., Li, F., Pingguan-Murphy, B., Bai, D., Xu, F., 2017. Trac Trend. Anal. Chem. 93, 37-50.

Drummond, T.G., Hill, M.G., Barton, J.K., 2003. Nat. Biotechnol. 21(10), 1192-1199.

Du, Y., Dong, S., 2016. Anal.Chem. 89(1), 189-215.

Gan, X., Zhao, H., Quan, X., 2017. Biosens. Bioelectron . 89, 56-71.

Ha, H.D., Han, D.J., Choi, J.S., Park, M., Seo, T.S., 2014. Small 10(19), 3858-3862.

Huang, Y., Zheng, W., Qiu, Y., Hu, P., 2016. ACS Appl. Mater. Inter. 8(35), 23362-23370.

Kawde, A.N., Wang, J., 2004. Electroanal. 16(1-2), 101-107.

Kim, B., Lee, J., Namgung, S., Kim, J., Park, J.Y., Lee, M., Hong, S., 2012. Sens.Actuators. B 169, 182-187.

Lee, D., Lee, J., Sohn, I.Y., Kim, B., Son, Y.M., Bark, H., Jung, J., Choi, M., Kim, T.H., Lee, C., Lee, N., 2015. Nano Res. 8(7), 2340-2350.

Li, Z., Chen, Y., Li, X., Kamins, T.I., Nauka, K., Williams, R.S., 2004. Nano Lett. 4(2), 245-247.

Liao, T., Li, X., Tong, Q., Zou, K., Zhang, H., Tang, L., Sun, Z., Zhang, G., 2017. Anal. Chem. 89(10), 5511-5518.

Mak, K.F., Lee, C., Hone, J., Shan, J., Heinz, T.F., 2010. Phys. Rev. Lett. 105(13), 136805.

Nam, H., Oh, B., Chen, M., Wi, S., Li, D., Kurabayashi, K., Liang, X., 2015. J. Vac. Sci. Technol. B 33(6), 1F-6F.

Naylor, C.H., Kybert, N.J., Schneier, C., Xi, J., Romero, G., Saven, J.G., Liu, R., Johnson, A.T.C., 2016. ACS Nano 10(6), 6173-6179.

Pan, Z.W., Dai, Z.R., Wang, Z.L., 2001. Science 291(5510), 1947-1949.

Park, B.H., Oh, S.J., Jung, J.H., Choi, G., Seo, J.H., Kim, D.H., Lee, E.Y., Seo, T.S., 2017. Biosens. Bioelectron . 91, 334-340.

Peng, F., Su, Y., Zhong, Y., Fan, C., Lee, S., He, Y., 2014. Chem. Res. 47(2), 612-623.

Radisavljevic, B., Radenovic, A., Brivio, J., Giacometti, I.V., Kis, A., 2011. Nat. Nanotechnol. 6(3), 147-150.

Sanchez, V.C., Jachak, A., Hurt, R.H., Kane, A.B., 2011. Chem.Res.Toxicol. 25(1), 15-34.

Sarkar, D., Liu, W., Xie, X., Anselmo, A.C., Mitragotri, S., Banerjee, K., 2014. ACS Nano 8(4), 3992-4003.

Sassolas, A., Leca-Bouvier, B.D., Blum, L.J., 2008. Chem. Rev. 108(1), 109-139.

Song, H., Ni, Y., Kokot, S., 2014. Biosens. Bioelectron. 56, 137-143.

Sozzi, G., Musso, K., Ratcliffe, C., Goldstraw, P., Pierotti, M.A., Pastorino, U., 1999. Clin. Cancer Res. 5(10), 2689-2692.

Summerton, J., 1989. Woodlands, TX, 71-80.

Summerton, J., WELLER, D., 1997. 7(3), 187-195.

Summerton, J.E., 2006. Morpholinos and PNAs Compared. In: Peptide Nucleic Acids, Morpholinos and Related Antisense Biomolecules. Medical Intelligence Unit. Springer, Boston, MA.

Tan, C., Cao, X., Wu, X., He, Q., Yang, J., Zhang, X., Chen, J., Zhao, W., Han, S., Nam, G., 2017. Chem. Rev. 117(9), 6225-6331.

Tang, R., Yang, H., Choi, J.R., Gong, Y., You, M., Wen, T., Li, A., Li, X., Xu, B., Zhang, S., 2017. Crit. Rev. Cl. Lab. Sci. 54(5), 294-308.

Tang, R., Yang, H., Gong, Y., You, M., Liu, Z., Choi, J.R., Wen, T., Qu, Z., Mei, Q., Xu, F., 2017. Lab Chip. 17(7), 1270-1279.

Turner, A.P., 2013. Chem. Soc. Rev. 42(8), 3184-3196.

Wang, J., 2003. Anal. Chem. Acta. 500(1), 247-257.

Wang, J., 2005. Electroanal. 17(1), 7-14.

Wang, L., Wang, Y., Wong, J.I., Palacios, T., Kong, J., Yang, H.Y., 2014. Small 10(6), 1101-1105.

Wang, Q.H., Kalantar-Zadeh, K., Kis, A., Coleman, J.N., Strano, M.S., 2012. Nat. Nanotechnol. 7(11), 699-712.

Watson, J.D., Crick, F.H., 1953. Nature 171(4356), 737-738.

Wu, S., Zeng, Z., He, Q., Wang, Z., Wang, S.J., Du, Y., Yin, Z., Sun, X., Chen, W., Zhang, H., 2012. Small 8(14), 2264-2270.

Yager, P., Domingo, G.J., Gerdes, J., 2008. Annu. Rev. Biomed. Eng. 10, 107-144.

Yuan, J., Wu, S., Duan, N., Ma, X., Xia, Y., Chen, J., Ding, Z., Wang, Z., 2014. Talanta 127, 163-168.

Zeng, Z., Yin, Z., Huang, X., Li, H., He, Q., Lu, G., Boey, F., Zhang, H., 2011. Angew. Chem. Int. Ed. 50(47), 11093-11097.

Zhang, G., Luo, Z.H.H., Huang, M.J., Tay, G.K.I., Lim, E.A., 2010. Biosens. Bioelectron. 25(11), 2447-2453.

Zhang, H., 2015. ACS Nano 9(10), 9451-9469.

Zheng, C., Huang, L., Zhang, H., Sun, Z., Zhang, Z., Zhang, G., 2015. ACS Appl. Mater. Inter. 7(31), 16953-16959.

Zhou, G., Chang, J., Pu, H., Shi, K., Mao, S., Sui, X., Ren, R., Cui, S., Chen, J., 2016. ACS Sens. 1(3), 295-302.

Figure captions:

Figure 1. Schematic illustration of the MoS_2 FET biosensor for detection of DNA based on PMO-DNA hybridization.

Figure 2. (a) SEM image of MoS_2 nanosheet spanning across Au electrodes. (b) AFM image of the as-fabricated MoS_2 FET device, lines A-B, C-D represent the measuring line and height profiles from the two lines of the AFM image.

Figure 3. (a) Transfer characteristic curve of the bare MoS_2 on a SiO_2/Si substrate (I_{ds} = 0.1 V). (b) Output characteristics curve of the MoS_2 FET device. The gate voltage (V_g) is varied from 0 to 0.3V with an interval of 0.1 V.

Figure 4. (a) Transfer characteristics of the PMO-functionalized MoS_2 FET device hybridized with the complementary DNA at a series of concentrations from 10 fM to 1 nM. Inset: the linear regime of the transfer characteristics curves (V_g=-0.1~0.1V). (b) The working curve of the MoS_2 FET biosensors for detection of DNA. Dashed line represents the triple noise level (~4.5%) from the blank control test.

Figure 5. (a) The linear regime of the transfer characteristics of a PMO-functionalized MoS_2 FET biosensor incubated with 0.5×PBS buffer solution, as a blank control, 1 nM non-complementary DNA, 1 nM one-base mismatched DNA and 1 nM three-base mismatched DNA, respectively. (b) Summary of $\Delta I_{ds}/I_{ds0}$ shifts of the MoS_2 FET biosensor: 0.5× PBS buffer solution , 1 nM non-complementary DNA , 1 nM one-base mismatched DNA , 1 nM three-base mismatched DNA and 1 pM complementary DNA.

Figure 6. The change of $\Delta I_{ds}/I_{ds0}$ of the PMO-immobilized MoS_2 FET biosensors for detecting target complementary DNA in 10×diluted serum samples.

Figure 1

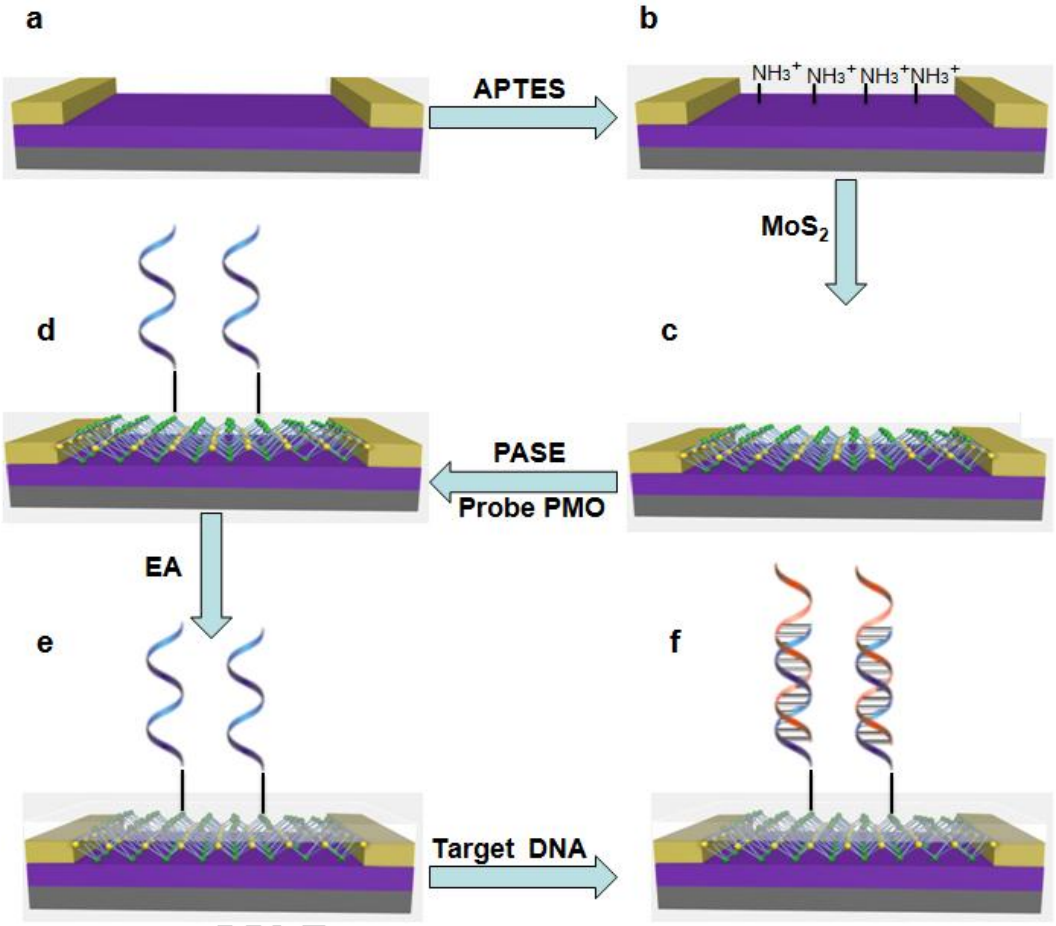

Figure 2

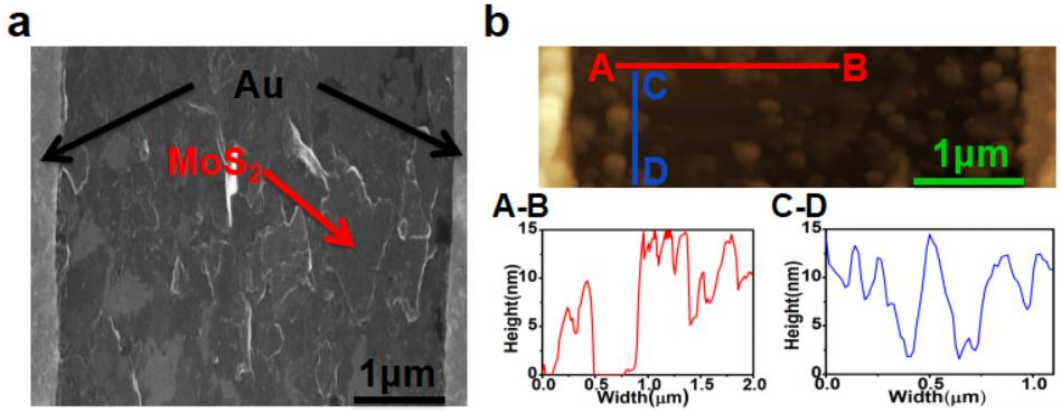

Figure 3

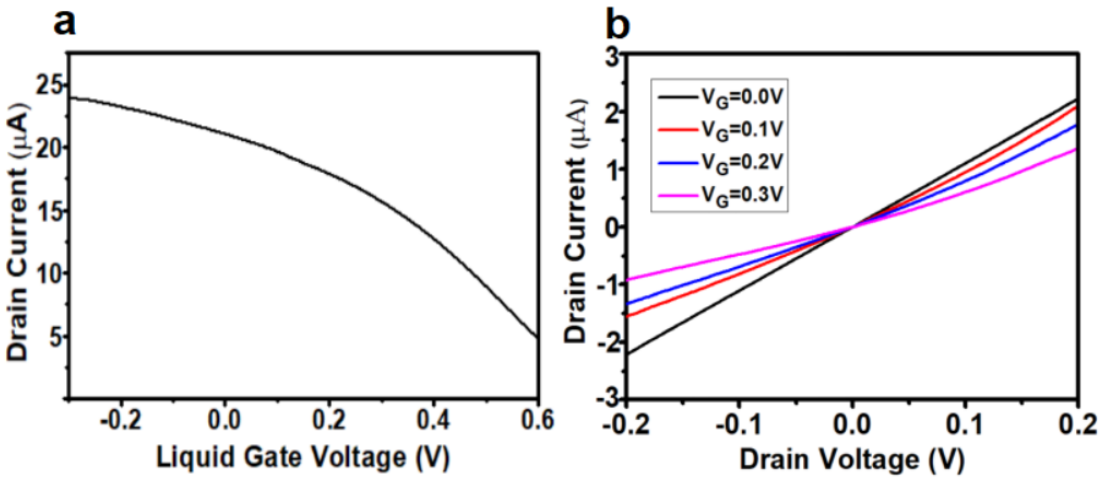

Figure 4

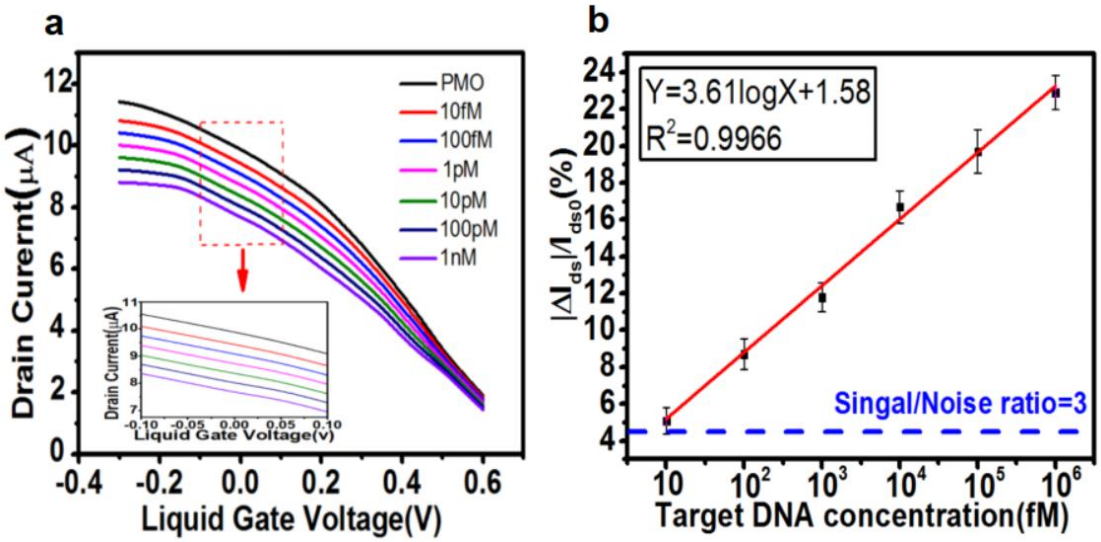

Figure 5

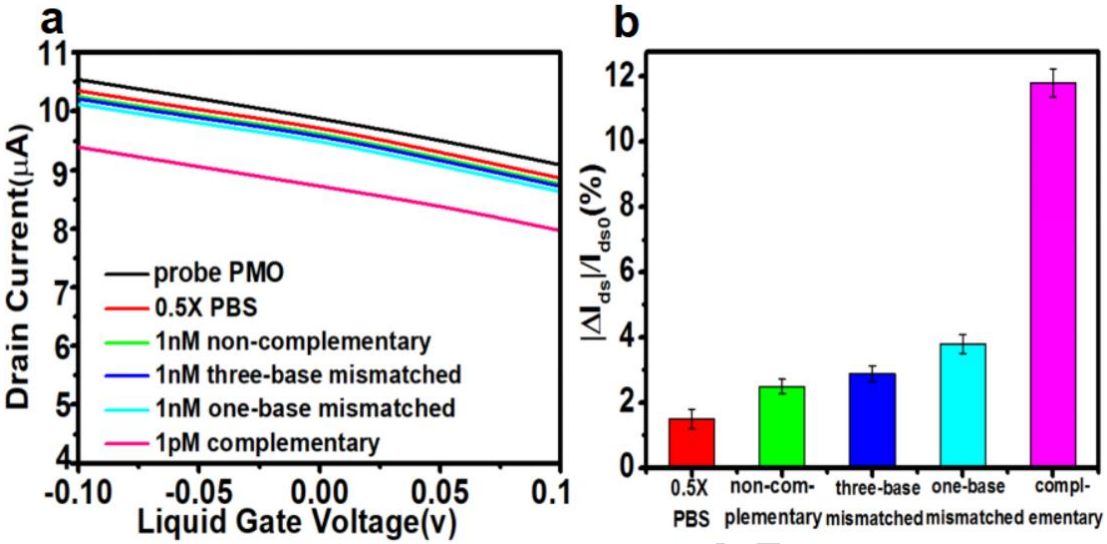

Figure 6

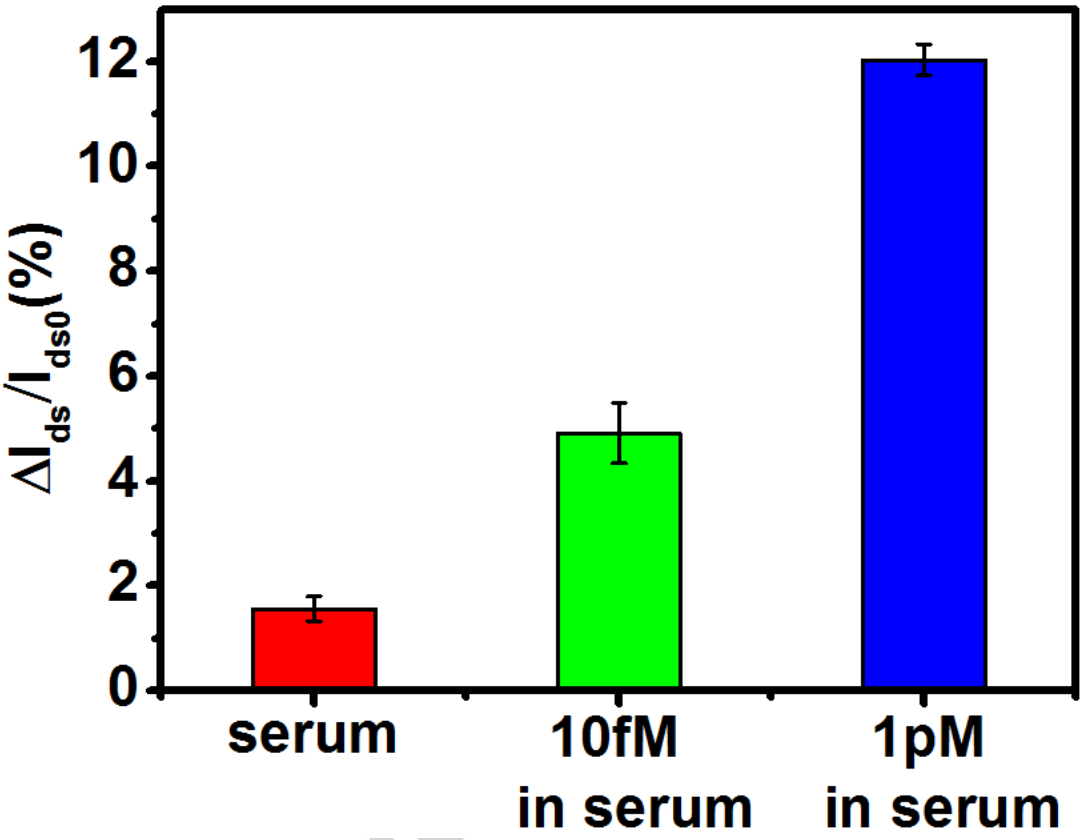

Highlights

1. DNA detection is realized by a MoS_2 based FET biosensor.
2. PMO-DNA hybridization is employed for the detection.
3. The FET biosensor is able to detect DNA in complex sample.
4. High sensitivity is achieved by using PMO as probe .
5. The developed sensing method shows satisfactory specificity.